

University of Mississippi

eGrove

---

Honors Theses

Honors College (Sally McDonnell Barksdale  
Honors College)

---

2011

## A Comparison and Cooperative Utilization of Møller–Plesset perturbation theory and B3LYP Density Functional Theory on Weakly Bound Structures

Joshua Ryan Smith

Follow this and additional works at: [https://egrove.olemiss.edu/hon\\_thesis](https://egrove.olemiss.edu/hon_thesis)

---

### Recommended Citation

Smith, Joshua Ryan, "A Comparison and Cooperative Utilization of Møller–Plesset perturbation theory and B3LYP Density Functional Theory on Weakly Bound Structures" (2011). *Honors Theses*. 2124.  
[https://egrove.olemiss.edu/hon\\_thesis/2124](https://egrove.olemiss.edu/hon_thesis/2124)

This Undergraduate Thesis is brought to you for free and open access by the Honors College (Sally McDonnell Barksdale Honors College) at eGrove. It has been accepted for inclusion in Honors Theses by an authorized administrator of eGrove. For more information, please contact [egrove@olemiss.edu](mailto:egrove@olemiss.edu).

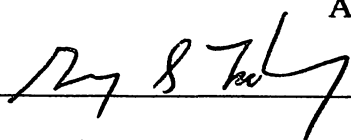
A Comparison of Second Order Møller–Plesset Perturbation Theory and the B3LYP Density  
Functional Theory for the Geometry Optimization of Water Clusters and the Formic Acid  
Tetramer

By – Joshua Ryan Smith

A thesis submitted to the faculty of the University of Mississippi in partial fulfillment of the  
requirements of the Sally McDonnell Barksdale Honors College

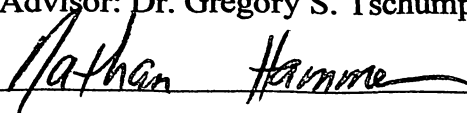
Oxford 2011

Approved by:



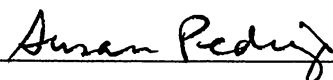
---

Advisor: Dr. Gregory S. Tschumper



---

Reader: Dr. Nathan Hammer



---

Reader: Dr. Susan Pedigo

*To my beautiful wife and my loving family, who believe I am capable of anything.*

## ACKNOWLEDGEMENTS

I would like to acknowledge the Mississippi Center for Super Computing Research for CPU time. This work was financially supported by the National Science Foundation (CHE-0957317 and EPS-0903787). GST has also received additional support through Oak Ridge National Laboratory Managed by UT Battelle, LLC under Contract No. De-AC05-00OR22725 for the U.S. Department of Energy.

I would also like to thank Dr. Tschumper for allowing me the opportunity to conduct research for this study, as well as his patience, direction, and instruction throughout this process. In addition, I would like to thank Kari Copeland and Desiree Bates for offering copious amounts of time helping me grasp and understand computational chemistry. I would also like to thank Dr. Pedigo for showing me how to think about biochemistry. I would also like to thank Dr. Hammer for generously helping in preparing my presentation. Lastly, I would like to thank both Dr. Hammer and Dr. Pedigo for being readers for my thesis.

## ABSTRACT

The B3LYP density functional was used along with a 6-31+G(*d,2p*) basis set to determine the optimal (energy minimized) geometries of more than 70 water clusters, ranging from (H<sub>2</sub>O)<sub>3</sub> to (H<sub>2</sub>O)<sub>10</sub>, and 11 formic acid tetramers. This approach was compared to high level benchmark structures obtained from second-order Møller-Plesset perturbation theory (MP2) on calculations with a correlation consistent triple-zeta basis set denoted as haTZ (cc-pVTZ for H and aug-cc-pVTZ of O and C). The two metrics of comparison were root mean square (RMS) geometric deviation between the B3LYP and MP2 fully optimized structures, and the associated energetic error on the MP2/haTZ potential energy surface (PES). The energetic error was obtained by comparing the MP2/haTZ single point energy of a particular B3LYP optimized structure (i.e. MP2/haTZ//B3LYP/6-31+G(*d,2p*)) to that of the corresponding MP2/haTZ optimized structure (i.e. MP2/haTZ//MP2/haTZ). Energetically, B3LYP produced water structures that deviated by an average of only 0.21 kcal mol<sup>-1</sup> from the MP2/haTZ benchmark geometries. In addition the average error for formic acid is 1.05 kcal mol<sup>-1</sup>. The root mean square deviations (RMSD) between unweighted Cartesian coordinates of the B3LYP/6-31+G(*d,2p*) and MP2 optimized structures for water was 0.033 Å, and for formic acid it was 1.05 Å.

## PREFACE

The science reported here was carried out from January 2009 to March 2011.

## Table of Contents

<b>I. Introduction and Theory</b>	7
<b>II. Methods</b>	8
<b>III. Results</b>	9
<b>IV. Conclusions</b>	11
<b>References</b>	21

## I. Introduction

Noncovalent interactions are important in many facets of the chemistry of living organisms. For instance, hydrogen bonding dictates the structure and physical properties of many systems, ranging from water clusters to DNA.<sup>1</sup> In addition, hydrogen bonding is responsible for the bonding between nucleotide bases, which govern biological information regarding heredity, genotypes, and genetic diversity. Hydrogen bonding is also pivotal in biochemical macromolecular structures. For example, hydrogen bonding helps determine the three dimensional shape associated with the secondary, tertiary, and quaternary structure of proteins.

Weakly-bound systems are governed by noncovalent interactions. Noncovalent interactions can take the form of hydrogen bonding, electrostatic interactions, van der Waals forces,  $\pi$ -type interactions, and many more. The conventional definition of hydrogen bonding is typically inferred by examining the physical properties between similar systems such as found between water and hydrogen sulfide.<sup>2</sup> Water has been widely used as a model, due to its significance in life processes, as well as its unique physical properties which is due to its ability to form an interconnected hydrogen bonding network.<sup>3</sup>

The formic acid tetramer is studied in this work because, in addition to hydrogen bonding,  $\pi$ -type dispersion interactions are a significant component of the binding energy. This is due to the fact that formic acid tetramers are held together by both hydrogen bonds, and dispersion forces. Formic acid clusters are also useful models for various biochemical processes, such as proton transfer.<sup>4</sup>

Geometrical optimizations allow exploration into the molecular structures of the clusters under study. A geometry optimization calculation attempts to find the lowest energetic point on



the potential energy surface (PES) for a particular molecular system. A simple example of geometry optimization is the bonding that occurs between atoms in the diatomic  $H_2$  molecule. As hydrogen molecules become too close or too far apart, their energy increases, making them unstable geometric isomers. However, at the optimal intermolecular distance the system has the lowest energy on the PES. Consequently, the process of computing that point on the PES is referred to as a geometry optimization or energy minimization.

Accurate optimized geometries can be obtained with benchmark calculations that are known to yield reliable structures based on extensive calibration. A widely-used benchmark method of geometry optimization of weakly bound systems is second order Møller–Plesset perturbation theory (MP2) and at least high quality triple-zeta basis set with several sets of diffuse and polarization functions.<sup>5-7</sup>

Density Functional Theory (DFT) is a less computationally expensive method. B3LYP is, by far, the most commonly used DFT method because it generally provides a very reasonable description of the ground state energies, geometries, and properties for a wide range of molecular systems. This theory tends to be less accurate than MP2, but it can be applied to larger systems.<sup>8-9</sup>

## II. Computational Methods

All clusters were optimized with the MP2 method and the B3LYP functional. MP2 optimizations were performed with a triple- $\zeta$  basis set, cc-pVTZ for H and aug-cc-pVTZ for O and C, denoted haTZ. The B3LYP calculations utilized the 6-31+G(*d*,2*p*) basis set and a grid having 99 radial shells and 590 angular points per shell. Residual Cartesian gradients for structures that were optimized were at least  $4.5 \times 10^{-4} E_h \text{ bohr}^{-1}$ . For all MP2 calculations the 1s like core orbitals of the oxygen atoms were frozen. All calculations were performed with

Gaussian03,<sup>10</sup> Gaussian09<sup>11</sup> and MPQC<sup>12</sup> software packages. The initial Cartesian coordinates for all the water structures under study can be found in References 9, 13, 14 and 15. In addition the initial formic acid structures were taken from Reference 4.

Two systemically different metrics were used in analysis to compare the two computational methods; geometry and energetics. Geometrically, the water and formic acid structures were analyzed using TINKER<sup>16</sup> software. The software determines the unweighted root mean square (RMS) deviation between the Cartesian coordinates of the B3LYP/6-31+G(*d*,2*p*) and the MP2/haTZ optimized structures. The optimized structures are superimposed using an algorithm that maximizes the overlap, thereby determining the geometric discrepancies between the two structures.

Energetically, MP2/haTZ single point energy calculations were taken of the B3LYP/6-31+G(*d*,2*p*) optimized structures. The MP2/haTZ optimized structure corresponded to the lowest point associated with a particular minimum on the MP2/haTZ PES. The B3LYP/6-31+G(*d*,2*p*) structures lie above this minimum. B3LYP/6-31+G(*d*,2*p*) optimization structures that accurately produce the MP2/haTZ energies will be close to the bottom of the well, and will have the smallest deviation from the MP2/haTZ//MP2/haTZ cluster energy.

### III. Results and Discussion

Because the number of possible conformational isomers grows quickly with *n*, only structures within 5 kcal mol<sup>-1</sup> of the lowest lying isomer were examined in this study. Table I contains both the RMS deviations of the unweighted Cartesian coordinates, as well as the associated energetic error of water clusters relative to MP2/haTZ for MP2/haTZ//B3LYP/6-31+G(*d*,2*p*) structures. The RMS deviation of B3LYP/6-31+G(*d*,2*p*) is generally quite small and never exceeds 0.184 Å for the Noncubic1 isomer of (H<sub>2</sub>O)<sub>8</sub>. Similarly, the ΔE values never

exceed  $0.44 \text{ kcal mol}^{-1}$  for the OB2 and OB3 isomer of  $(\text{H}_2\text{O})_{10}$ . Table II is a statistical analysis of RMSD and  $\Delta E$  values found in Table I. Both the energetic error ( $\Delta E$ ) and the structural errors (RMSD) tend to increase with the size of the water cluster. For this set of 76  $(\text{H}_2\text{O})_n$  structures, the B3LYP/6-31+G(*d,2p*) structures deviate from the MP2/haTZ ones on average by a few hundredths of an Å and by just a couple of tenths of a  $\text{kcal mol}^{-1}$  on average on the MP2/haTZ structure.

Table III contains a similar set of data for the formic acid tetramer structures. Results for the CA, CZ, PA1, PA2 and PA3 structures are quite similar.  $\Delta E$  values are on the order of a few tenths of a  $\text{kcal mol}^{-1}$ , and the RMS deviations are on the order of a few hundredths of an Å. The errors associated with the B3LYP/6-31+G(*d,2p*) optimizations of the other structures, however, are nearly an order of magnitude larger. The energetic errors exceed  $2 \text{ kcal mol}^{-1}$  and the RMS deviations grow as large as  $0.710 \text{ Å}$ . These two rather disparate sets of results yield average errors of  $1.05 \text{ kcal mol}^{-1}$  and  $0.218 \text{ Å}$  respectively, for the 11 formic acid tetramer structures examined in this study.

The contrasting errors can be understood by examining the difference between the structures of the two groups of formic acid tetramers. In the first group (with the small errors) of tetramers are essentially planar and are held together by a network of hydrogen bonds. (See, for example, structure PA1 in Figure 4.) The other group of structures (with the large errors), still contains hydrogen bonding but attractive  $\pi$ -type interactions between the  $\pi$  electron clouds of the formic acid molecules also stabilize the system. These interactions give rise to “stacked” structures such as the one in Figure 5. Like most DFT methods, the B3LYP functional does not include dispersions. Therefore, it is not surprising that B3LYP/6-31+G(*d,2p*) optimized structures have large errors for this second group of formic acid tetramer structures.

It should also be noted that in every case the largest relative error associated with the calculation of MP2/haTZ energies using B3LYP/6-31+G(*d,2p*) optimized (H<sub>2</sub>O)<sub>*n*</sub> structures was <1%. This good performance of the B3LYP/6-31+G(*d,2p*) model chemistry optimizations of water clusters may still not be adequate in certain pathological cases where water clusters are virtually isoenergetic and separated by a few tenths of a kcal mol<sup>-1</sup>. For example, the MP2 complete basis set interaction energies for the prism and cage isomers of the water hexamer are only electronically separated by 0.06 kcal mol<sup>-1</sup>.<sup>13</sup> B3LYP with the 6-31+G(*d,2p*) basis set is a good approach for finding low-lying water structures on the PES, but to reproduce energetics for low-lying clusters within a 0.20 kcal mol<sup>-1</sup> another methodology is necessary.

#### IV. Conclusion

The B3LYP/6-31+G(*d,2p*) method and basis set were utilized to optimize over 70 water structures, ranging from (H<sub>2</sub>O)<sub>3</sub> to (H<sub>2</sub>O)<sub>10</sub>, and 11 formic acid tetramer structures. In this application MP2/haTZ was used as the high level benchmark calculation to which the B3LYP/6-31+G(*d,2p*) method was compared to. This comparison involved two different metrics, the minimum RMS deviation of unweighted Cartesian coordinates and the MP2/haTZ electronic energy.

The B3LYP/6-31+G(*d,2p*) optimized structures performed well geometrically for water, only allowing an RMS deviation of 0.033 Å on average. Therefore, B3LYP/6-31+G(*d,2p*) is effective for determining geometry of (H<sub>2</sub>O)<sub>*n*</sub> clusters because they are electromagnetically dominant. However, formic acid performed poorly, with an average RMS deviation of 0.218 Å. This value is larger than the maximum RMS deviation associated with water, which is found at 0.184 Å. These large differences are likely due to the significant role dispersion forces play in the stacked structures, which is not accounted for by the B3LYP method. These structural

deviations of the B3LYP/6-31+G(*d,2p*) optimized geometries correspond to energetic errors on the MP2/haTZ PES of just a few tenths of a kcal mol<sup>-1</sup> of the water clusters, but over 1 kcal mol<sup>-1</sup> of the formic acid tetramer.

The B3LYP/6-31+G(*d,2p*) method is a very effective approach for optimizing low-lying stationary points of (H<sub>2</sub>O)<sub>*n*</sub> clusters and planar formic acid structures. It does not, however, reliably describe the stacked structures of the formic acid tetramer in which  $\pi$ -type interactions play a significant role.

Despite the overall good performance of this relatively efficient method for water clusters, it is not always accurate enough to resolve the relative ordering of the low-lying (H<sub>2</sub>O)<sub>*n*</sub> isomers. Future research should be based upon finding methods capable of supplying more accurate structures within 0.1 kcal mol<sup>-1</sup> for a diverse range of weakly bound, noncovalent clusters, not just water. This new approach must also be efficient enough to be routinely applied to large clusters.

Table 1: Errors (in kcal mol<sup>-1</sup>) relative to  $\Delta E$  MP2/haTZ for MP2/haTZ //B3LYP/6-31+G(*d,2p*) structures, and RMS Deviation (in Å) of B3LYP/6-31+G(*d,2p*) relative to MP2/haTZ optimized structures

(H <sub>2</sub> O) <sub>n</sub>	MP2/haTZ	Error $\Delta E$	RMS D
<b>(H<sub>2</sub>O)<sub>3</sub></b>			
C <sub>1</sub>	15.91	0.10	0.010
C <sub>3</sub>	15.16	0.11	0.012
C <sub>3h</sub>	14.57	0.10	0.009
<b>(H<sub>2</sub>O)<sub>4</sub></b>			
C <sub>4h</sub>	28.01	0.16	0.012
C <sub>4</sub>	27.08	0.16	0.010
S <sub>4</sub>	25.83	0.14	0.017
C <sub>i</sub>	24.97	0.15	0.010
<b>(H<sub>2</sub>O)<sub>5</sub></b>			
C <sub>1</sub>	36.79	0.19	0.041
C <sub>5</sub>	34.04	0.21	0.014
C <sub>5h</sub>	33.43	0.22	0.018
<b>(H<sub>2</sub>O)<sub>6</sub></b>			
Prism	46.65	0.25	0.031
Cage	46.64	0.26	0.040
Book1	46.34	0.23	0.019
Book2	46.04	0.25	0.081
Bag	45.47	0.24	0.055
Cyclic Chair	45.41	0.23	0.017
Cyclic Boat1	44.41	0.25	0.078
Cyclic Boat2	44.32	0.25	0.080
<b>(H<sub>2</sub>O)<sub>7</sub></b>			
A	58.40	0.30	0.036
Pr2	58.03	0.31	0.047
Pr3	57.84	0.30	0.036
Ca1	56.86	0.28	0.029
B	56.82	0.29	0.039
Ca2	56.03	0.28	0.025
CH2	55.41	0.27	0.043
CH1	55.05	0.28	0.101
CH3	55.05	0.28	0.106
C	54.92	0.28	0.046
BI1	54.89	0.25	0.019
D	54.82	0.25	0.048
<b>(H<sub>2</sub>O)<sub>8</sub></b>			
D <sub>2d</sub>	74.08	0.35	0.024
S <sub>4</sub>	74.05	0.36	0.026
C <sub>2</sub>	71.14	0.39	0.050
C <sub>i</sub>	71.09	0.35	0.031
C <sub>s</sub>	70.22	0.35	0.032
C <sub>1b</sub>	70.06	0.35	0.030

C <sub>1a</sub>	69.95	0.34	0.029
C <sub>1c</sub>	69.89	0.35	0.029
Noncubic 1	69.23	0.41	0.184
<hr/>			
(H <sub>2</sub> O) <sub>9</sub>			
D <sub>2d</sub> DDh	83.57	0.38	0.025
S <sub>4</sub> DAh-1	83.31	0.38	0.024
S <sub>4</sub> DAh-2	83.31	0.38	0.025
S <sub>4</sub> DDh-1	83.21	0.39	0.026
S <sub>4</sub> DDh-2	83.22	0.39	0.025
D <sub>2d</sub> DAh	83.05	0.37	0.022
S <sub>4</sub> DAnh-1	83.05	0.38	0.023
S <sub>4</sub> DAnh-2	82.91	0.38	0.024
<hr/>			
(H <sub>2</sub> O) <sub>10</sub>			
PP2	95.12	0.43	0.027
PP1	95.07	0.38	0.026
PP3	95.06	0.41	0.028
PP4	94.56	0.40	0.026
PP5	94.51	0.43	0.026
OB1	94.47	0.43	0.028
DP2	93.58	0.43	0.037
OB2	93.58	0.44	0.028
OB3	93.50	0.44	0.028
DP1	93.48	0.41	0.034
OB11	93.22	0.43	0.026
OB4	93.17	0.42	0.026
OB6	93.16	0.43	0.033
OB5	93.06	0.43	0.033
OB7	93.04	0.43	0.032
OB8	92.85	0.42	0.060
DP3	92.85	0.37	0.102
DP4	92.70	0.29	0.050
DP7	92.60	0.41	0.052
DP6	92.59	0.41	0.012
OB9	92.54	0.43	0.032
DP5	92.51	0.37	0.031
DP10	92.48	0.33	0.035
DP8	92.43	0.37	0.119
OB10	92.29	0.07	0.065
DP11	92.28	0.41	0.033
C1	92.05	0.41	0.039
C2	90.85	0.40	0.022
C3	90.72	0.41	0.010

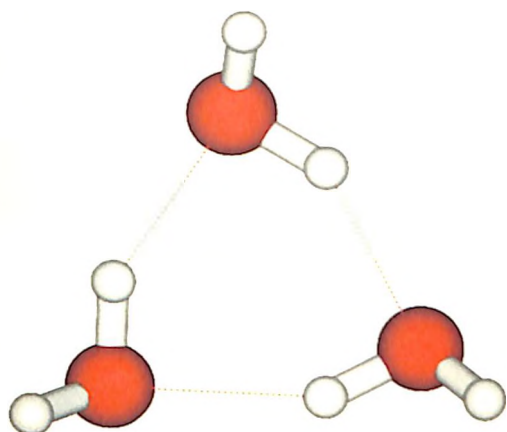
Table II: Average and maximum RMS deviations (in Å) for B3LYP/6-31+G(*d,2p*) relative to MP2/haTZ optimized structures, and average errors (in kcal mol<sup>-1</sup>) relative to ΔE MP2/haTZ for MP2/haTZ //B3LYP/6-31+G(*d,2p*) structures, for various (H<sub>2</sub>O)<sub>*n*</sub> clusters with *n*=3-10.

(H <sub>2</sub> O) <sub><i>n</i></sub>	#	Avg ΔE	Max ΔE	Avg RMSD	Max RMSD
(H <sub>2</sub> O) <sub>3</sub>	3	0.11	0.11	0.010	0.012
(H <sub>2</sub> O) <sub>4</sub>	4	0.15	0.16	0.012	0.017
(H <sub>2</sub> O) <sub>5</sub>	3	0.21	0.22	0.024	0.041
(H <sub>2</sub> O) <sub>6</sub>	8	0.24	0.26	0.048	0.081
(H <sub>2</sub> O) <sub>7</sub>	12	0.28	0.31	0.048	0.106
(H <sub>2</sub> O) <sub>8</sub>	9	0.36	0.41	0.048	0.184
(H <sub>2</sub> O) <sub>9</sub>	8	0.38	0.39	0.024	0.026
(H <sub>2</sub> O) <sub>10</sub>	29	0.40	0.44	0.040	0.119
All	76	0.21	0.44	0.033	0.184

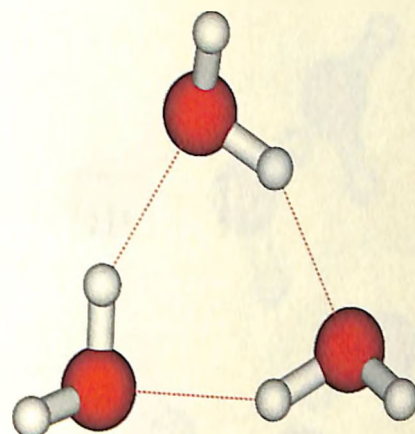
Table III: Average and maximum RMS deviations (in Å) for B3LYP/6-31+G(*d,2p*) relative to MP2/haTZ optimized structures, and average errors (in kcal mol<sup>-1</sup>) relative to ΔE MP2/haTZ for MP2/haTZ //B3LYP/6-31+G(*d,2p*) structures, for various formic acid tetramers

Tetramer	MP2/haTZ	Error ΔE	RMS D
As2	38.29	1.49	0.252
As3	38.21	1.75	0.281
SS1	38.19	1.38	0.710
As1	37.97	2.04	0.321
B1	37.65	1.99	0.315
B2	37.06	1.60	0.289
PA1	36.57	0.21	0.038
PA2	36.21	0.21	0.054
CE	36.02	0.32	0.044
PA3	35.80	0.22	0.059
CZ	32.30	0.32	0.036
Average	-	1.05	0.218





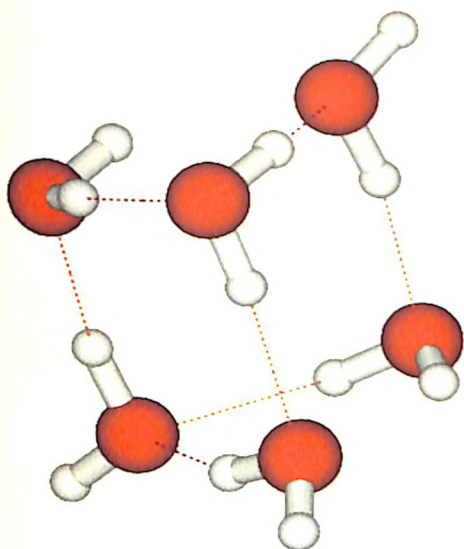
C3 B3LYP



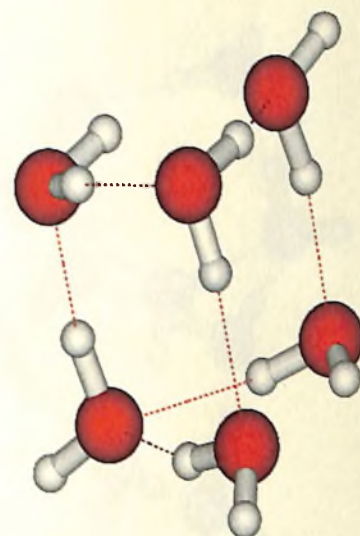
C3 MP2

RMS Deviation 0.012 angstroms and  $\Delta E$  0.11 kcal mol<sup>-1</sup>

**Figure 1:** Water Trimer C<sub>3</sub> Geometries and Energetics



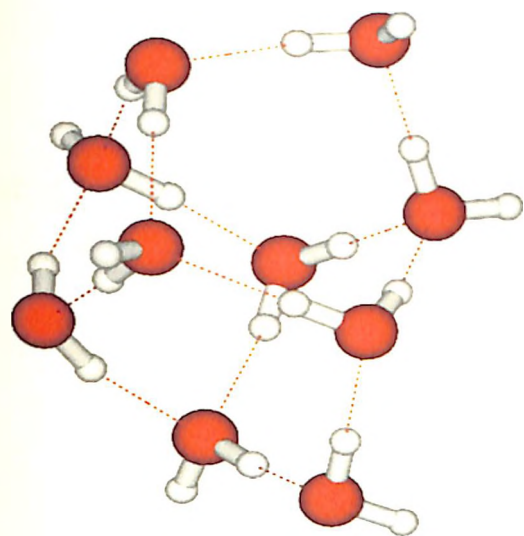
Prism B3LYP



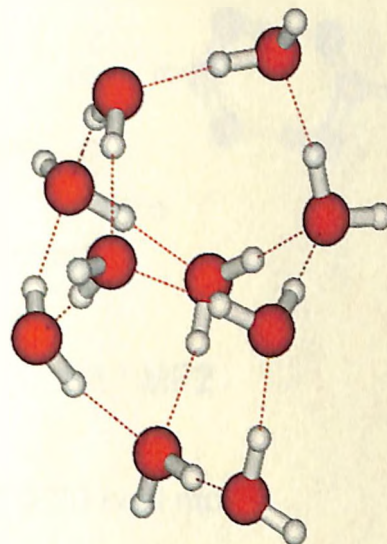
Prism MP2

RMS Deviation 0.031 Å and  $\Delta E$  0.25 kcal mol<sup>-1</sup>

**Figure 2:** Water Hexamer (Prism) Geometries and Energetics



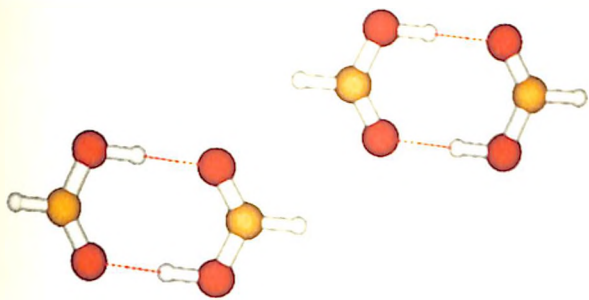
DP8 B3LYP



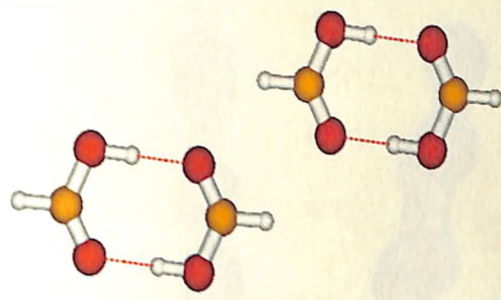
DP8 MP2

RMS Deviation 0.119 Å and  $\Delta E$  0.37 kcal mol<sup>-1</sup>

**Figure 3:** Water Decamer (DP8) Geometries and Energetics



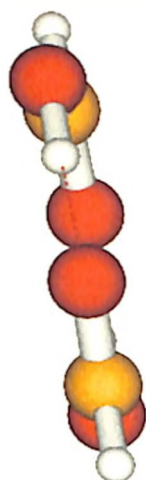
PA1 B3LYP



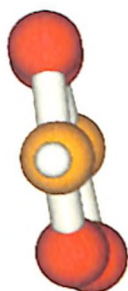
PA1 MP2

RMS Deviation 0.038 Å and  $\Delta E$  0.20 kcal mol<sup>-1</sup>

**Figure 4:** Formic Acid (PA1) Geometries and Energetics



SS1 B3LYP



SS1 MP2

RMS Deviation 0.710 Å and  $\Delta E$  1.38 kcal mol<sup>-1</sup>

**Figure 5:** Formic Acid (SS1) Geometries and Energetics

## REFERENCES

1. J. Rezac, P. Hobza and S. A. Harris, *Biophys. J.* **98**, 101-110 (2010)
2. D. Hankins, J. W. Moskowitz and F. H. Stillinger, *J. Chem. Phys.* **53**, 4533-4544 (1970).
3. E. Arunan and S. Scheiner, "Categorizing hydrogen bonding and other intermolecular interactions." IUPAC, (2004). <http://www.iupac.org/web/ins/2004-026-2-100>
4. A. Karpfen and A. J. Thakkar, *J. Chem. Phys.* **124**, 22313 (2006).
5. J. K. Kazimirski and V. Buch, *J. Phys. Chem. A*, **107**, 9762-9775 (2003).
6. S. S. Xantheas, C. J. Burnham and R. J. Harrison, *J. Chem. Phys.* **116**, 1493-1499 (2002).
7. G. Rauhut, P. Pulay, and H. J. Werner, *J. Comp. Chem.* **19**, 1241-1254 (1998).
8. J. Tirado-Rives and W. L. Jorgensen, *J. Chem. Theory Comput.* **4**, 297-306 (2008).
9. E. E. Dahlke, R. M. Olson, H. R. Leverentz and D. G. Truhlar, *J. Phys. Chem. A*, **112**, 3976-3984 (2008).
10. M. J. Frisch, G. W. Trucks, H. B. Schlegel, G. E. Scuseria, M. A. Robb, J. R. Cheeseman, J. R. Montgomery, Jr., T. Vreven, K. N. Kudin, J. C. Burant, J. M. Millam, S. S. Iyengar, J. Tomasi, V. Barone, B. Mennucci, M. Cossi, G. Scalmani, N. Rega, G. A. Petersson, H. Nakat-suji, M. Hada, M. Ehara, K. Toyota, R. Fukuda, J. Hasegawa, M. Ishida, T. Nakajima, Y. Honda, O. Kitao, H. Nakai, M. Klene, X. Li, J. E. Knox, H. P. Hratchian, J. B. Cross, V. Bakken, C. Adamo, J. Jaramillo, R. Gomperts, R. E. Stratmann, O. Yazyev, A. J. Austin, R. Cammi, C. Pomelli, J. W. Ochterski, P. Y. Ayala, K. Morokuma, G. A. Voth, P. Salvador, J. J. Dannenberg, V. G. Zakrzewski, S. Dapprich, A. D. Daniels, M. C. Strain, O. Farkas, D. K. Malick, A. D. Rabuck, K. Raghavachari, J. B. Foresman, J. V. Ortiz, Q. Cui, A. G. Baboul, S. Clifford, J. Cioslowski, B. B. Stefanov, G. Liu, A. Liashenko, P. Piskorz, I. Komaromi, R. L. Martin, D. J. Fox, T. Keith, M. A. Al-Laham,

- C. Y. Peng, A. Nanayakkara, M. Challacombe, P. M. W. Gill, B. Johnson, W. Chen, M. W. Wong, C. Gonzalez, and J. A. Pople, "Gaussian 03, Revision E.01," Gaussian, Inc., Wallingford, CT, 2004.
11. M. J. Frisch, G. W. Trucks, H. B. Schlegel, G. E. Scuseria, M. A. Robb, J. R. Cheeseman, G. Scalmani, V. Barone, B. Mennucci, G. A. Petersson, H. Nakatsuji, M. Caricato, X. Li, H. P. Hratchian, A. F. Izmaylov, J. Bloino, G. Zheng, J. L. Sonnenberg, M. Hada, M. Ehara, K. Toyota, R. Fukuda, J. Hasegawa, M. Ishida, T. Nakajima, Y. Honda, O. Kitao, H. Nakai, T. Vreven, J. A. Montgomery, Jr., J. E. Peralta, F. Ogliaro, M. Bearpark, J. J. Heyd, E. Brothers, K. N. Kudin, V. N. Staroverov, R. Kobayashi, J. Normand, K. Raghavachari, A. Rendell, J. C. Burant, S. S. Iyengar, J. Tomasi, M. Cossi, N. Rega, J. M. Millam, M. Klene, J. E. Knox, J. B. Cross, V. Bakken, C. Adamo, J. Jaramillo, R. Gomperts, R. E. Stratmann, O. Yazyev, A. J. Austin, R. Cammi, C. Pomelli, J. W. Ochterski, R. L. Martin, K. Morokuma, V. G. Zakrzewski, G. A. Voth, P. Salvador, J. J. Dannenberg, S. Dapprich, A. D. Daniels, Ö. Farkas, J. B. Foresman, J. V. Ortiz, J. Cioslowski, and D. J. Fox, Gaussian, Inc., Wallingford CT, 2009.
12. C. L. Janssen, I. B. Nielsen, M. L. Leininger, E. F. Valeev, and E. T. Seidl, "The massively parallel quantum chemistry program (mpqc) version 2.3.1," Sandia National Laboratories, Livermore, CA, USA, <http://www.mpqc.org> (2004).
13. D. M. Bates and G. S. Tschumper, *J. Phys. Chem. A*, **113**, 3555-3559 (2009).
14. P. Qian, W. Song, L. Lu and Z. Yang, *Int. J. Quantum Chem.* **110**, 1923-1937 (2009)
15. R. M. Shields, B. Temelso, K. A. Archer, T. E. Morrell and G. C. Shields, *J. Phys Chem. A*, **114**, 11725-11737 (2010).

16. J. W. Ponder, "Tinker - Software Tools for Molecular Design, Version 5.1.09.

Washington University School of Medicine; Saint Louis, MO: 2009.